



Chemical Methodologies

journal homepage: <http://chemmethod.com>



Original Research article

On The Characterization, Use and Wastewater Detoxification Potential of Pyrolyzed *Moringaoleifera* Pods and Shells PART B: Sorption Isotherm, Kinetic, and Thermodynamic study

Adams Udoji Itodo*, Raymond Ahulle Wuana, Wombo Ngunan Patience

Department of Chemistry, Federal University of Agriculture Makurdi, Nigeria.

ARTICLE INFORMATION

Received: 29 October 2017
Received in revised: 12 February 2018
Accepted: 20 February 2018
Available online: 02 March 2018

DOI:
10.22631/chemm.2018.113853.1033

KEYWORDS

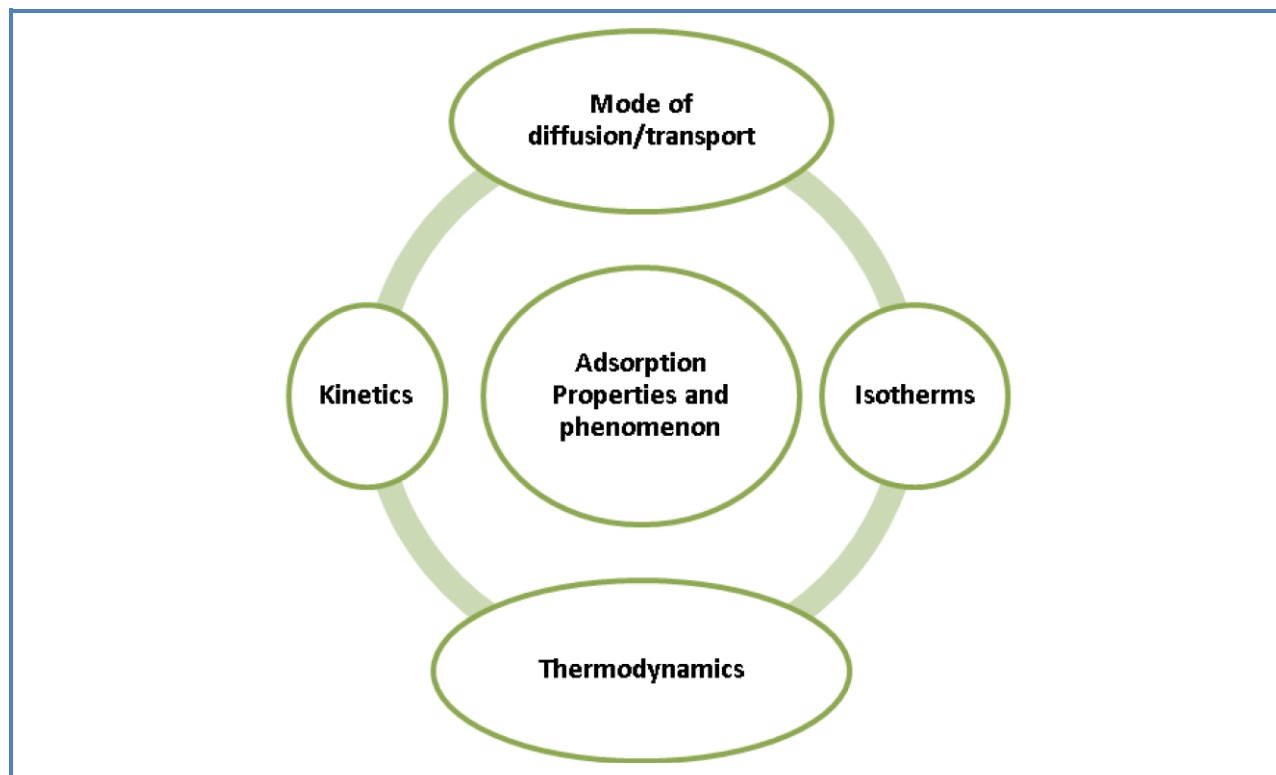
Diffusion
Isotherm
Rate
Equilibrium
Adsorption
Moringaoleifera

ABSTRACT

In this study, previously estimated tannery effluent with high pollutant (Cr) load of 987 mg/L was detoxified using pyrolysed *Moringaoleifera* Pods (PMOP) and Shells (PMOS). A performance assessment of the gained and characterized adsorbents was based on equilibrium, rate and thermodynamic studies. An investigation was carried out on equilibrium studies using isotherm models (Langmuir, Freundlich, Dubinin-Radushkevich and Temkin isotherm models). The maximum adsorption capacity of PMOS is 277.3 mg/g. Sorption rate is best explained using the Pseudo-second order kinetic model with diffusion through the liquid film surrounding the solid sorbent. Comparison of performance with commercially available activated carbon shows no statistical significance at $p < 0.05$.

*Corresponding author, email: itodoson2002@gmail.com; TEL. +2348039503463
Department of Chemistry, Federal University of Agriculture Makurdi, Nigeria

Graphical Abstract



Introduction

Contamination of tannery wastewater with organics and inorganics is a matter of concern which is linked to environmental impacts of tanning wastewater. Among the many pollutants, chrome tan wastewater consists of acidic and alkaline liquors with chromium levels of 100–400 mg/L [1]. Chromium in tannery is used to treat animal skin for leather. In chrome tanning process, trivalent chromium has the most common oxidation state [2], often in the form of Cr (III) sulfate [3]. For Collagen to react with Cr^{+3} ion, six coordination positions (octahedron) are available and stereoisomers are possible. Chromium III nitrate is thought to give a complex ion of the form $[\text{Cr}(\text{H}_2\text{O})_6]^{+3}$ in solution. Reaction sites for chrome tanning are the ionized carboxyl groups on side chains of the collagen [4]. Chromium is a very toxic metal. It is mutagenic as well as carcinogenic. In addition to that, it causes liver damage, lungs infection and skin irritations [5]. According to international standards, permitted limit of Cr (VI) for industrial effluents is 0.1 mg dm^{-3} .

Adsorption is one of the most effective and general wastewater treatment methods [6,7,8]. The adsorption technique is centered on the transfer of pollutants from the solution to the solid phase. Adsorption occurs if the attractive force between the solute and Adsorbent is greater than the cohesive energy of the substance itself. To maintain a favorable free-energy driving process (i.e. a

negative ΔG), the ΔH must be greater in magnitude than the $T\Delta S$, because adsorption leads to a loss of entropy (ΔS) [9].

The adsorption process is superior to any other method by its low cost, low energy requirement, the simplicity of design and possibility of reusing the spent adsorbent via regeneration. Adsorbents such as activated carbon available to remove contaminants from wastewaters are costly and hardly available [7,10]. Based on this, there is a need to study the effectiveness of uptake of pollutants on drawn adsorbents.

Moringaoleifera has gained importance due to its multipurpose use and well adaptability to dry and hot climates [11].The seed powder is used to treat water due to its curling capacity [12].The plant had been researched [11, 12,13].

Adsorption Models

Adsorption modeling is important to describe adsorbent-adsorbates [14].Adsorbate adsorbed per unit adsorbent mass is expressed as;

$$q_s = \frac{(C_0 - C_e)V}{W} \tag{1}$$

Isotherm models

Langmuir equation is expressed as:

$$\frac{C_e}{q_e} = \frac{1}{Q_m} C_e + \frac{1}{b \cdot Q_m} \tag{2}$$

Q_m and b , are estimated from the slope and intercept of the linear plot, C_e/q_e versus C_e . Other forms are shown in Table 1

Table 1. Linear Forms of Langmuir Isotherm Models

Forms	Plots
$\frac{C_e}{q_e} = \frac{1}{bQ_0} + \frac{C_e}{Q_0}$	$\frac{C_e}{Q_e}$ vs C_e
$\frac{C_e}{q_e} = \frac{1}{Q_0} + \frac{C_e}{bQ_0C_s}$	$\frac{1}{q_e}$ vs $\frac{1}{C_s}$
$q_s = Q_0 - \frac{q_s}{bC_s}$	q_s vs $\frac{q_s}{C_s}$
$\frac{q_s}{C_s} = bQ_0 - bq_s$	$\frac{q_s}{C_s}$ vs q_s

Freundlich isotherm model

Freundlich isotherm is described adsorption on a wide variety of adsorbents in the following the equation;

$$\log Q_s = \log K_f + \frac{1}{n} \log C_s \tag{3}$$

This isotherm takes on to incorporate the role of substrate-substrate on the surface [15,16]. Plotting $\log Q_e$ versus $\log C_e$ gives $1/n$ as slope and an intercept magnitude of $\log K_f$. Freundlich constants K_f and n are deduced from the intercept and slope of the linear plot. The smaller value of $1/n$ implies stronger interaction while $1/n$ equal to 1 is linear adsorption for uniform site energies.

Temkin isotherm model

Temkin isotherm assumes the heat of adsorption decreases linearly with the sorption coverage due to adsorbent-adsorbate [17]. Given as equation 4 is the linear form of Temkin isotherm:

$$q_s = \frac{RT}{b_T} \ln a_T + \frac{RT}{b_T} \ln C_s \quad (4)$$

R is universal gas constant (8.314 J/molK), T is temperature (K) and b_T (J/mol) is a constant related to the heat of sorption, R is the ideal gas constant (8.314 J/mol K). The slopes and intercept are obtained from the graphic plot q_s against $\ln C_s$ [18,19].

Dubinin-Rudushkevich isotherm model

According to Arasakumaret al. [17], Dubinin- Radushkevich curve is related to the porosity of the adsorbent. It expresses the adsorption occurring onto both homogeneous and heterogeneous surfaces. The linear form of the isotherm is

$$\ln q_s = \ln q_D - B \varepsilon^2 \quad (5)$$

The plot of $\ln(q_s)$ vs ε^2 tests the suitability of the data [20]. Important constants include the theoretical saturation capacity, q_D (mg/g); mean free energy of adsorption per mole of the adsorbate B (mol²/J²) and Polanyi potential, ε relates to equilibrium as:

$$\varepsilon = RT \ln(1 + C_s) \quad (6)$$

R is the Universal gas constant (8.314 J/mol/K) and T is the temperature in Kelvin. The mean energy, E is

$$E = \frac{1}{(2B)^{\frac{1}{2}}} \quad (7)$$

It is thus, possible to predict whether an adsorption is a physisorption or chemisorption.

Adsorption Kinetic Models

Lagergren equation (Pseudo-first order model)

The controlling mechanisms on adsorption [21], given a general and linear representation as equations 8 and 9 respectively

$$\frac{dq_t}{dt} = k_n (q_s - q_t) \quad (8)$$

$$\ln(1 - q_t/q_s) = -k_{fd} t \quad (9)$$

q_e and q_t are the adsorbate amount per unit mass of adsorbent (mgg^{-1}) at equilibrium and at time t , respectively, k_n suits the rate constant for n^{th} order adsorption.

Pseudo-second order model

The second model is also empirical [22] with the following linear expression.

$$\frac{t}{q_t} = \frac{1}{k_2 q_e^2} x \frac{t}{q_e} \quad (10)$$

Elovich model

It assumes a logarithmic time dependence of the adsorbed quantity. The governing equation in its linear form is:

$$Q = \frac{\ln(\alpha\beta) + \ln(t)}{\beta} \quad (11)$$

Where α ($\text{mg/g}^1/\text{min}^1$) and β (g/mg^1) are initial adsorption and desorption rate constants, respectively. Constant, α depicts rate of chemisorption and β is surface coverage [22]. A plot of q_t vs. $\ln(t)$ gives a slope and intercept of $(1/\beta)$ and $(1/\beta)\ln(\alpha\beta)$ respectively.

Intra-particle diffusion model (transport model)

Diffusion as a rate determinant was evaluated with intra-particle diffusion model.

$$q_t = K_{int} t^{1/2} \quad (12)$$

K_{int} is the intra-particle diffusion rate constant from plotting q_t vs. $t^{1/2}$ [23].

Film diffusion model

Film diffusion model is used to study the transport of metal ions from liquid phase to the solid phase boundary. The equation representing this model is:

$$\ln(1 - F) = -K_f t \quad (13)$$

Where F is the fractional attainment at equilibrium ($F = qt/q_e$), K_f is liquid film diffusion constant. Linear plot of the model is $\ln(1-F)$ versus t [24].

Adsorption Thermodynamics

Between the thermodynamic features; change in Gibb's free energy (ΔG^0), change in enthalpy ΔH^0 and change in entropy ΔS^0 is

$$\Delta G^0 = \Delta H^0 - T\Delta S^0 \quad (17)$$

According to the Van't Hoff expression; the process equilibrium constant varies with temperature.

$$\frac{d \ln K}{dT} = \frac{\Delta H}{RT^2} \quad (18)$$

$$\Delta G^0 = -RT \ln(K_{eq}) \quad (19)$$

$$\ln(K_{\text{eq}}) = \frac{\Delta S^{\circ}}{R} - \frac{\Delta H^{\circ}}{RT} \quad (20)$$

$$\ln(K_{\text{eq}}) = \alpha \frac{1}{T} \quad (21)$$

The method in a graphic is by a plot of $\ln(K_{\text{eq}})$ vs $\frac{1}{T}$

Where $\frac{\Delta H^{\circ}}{RT}$ and $\frac{\Delta S^{\circ}}{R}$ is the slope and intercept respectively [26]. K is the equilibrium constant, H is the enthalpy of reaction, T is the temperature in degree Celsius, K is equilibrium constant and R is the gas constant (8.314 J/mol).

Similarly, Arrhenius equation finds application in estimating thermodynamics

$$K = A \exp(E_a/RT) \quad (22)$$

$$\ln\left(\frac{K_1}{K_2}\right) = \frac{E_a}{R} \left(\frac{1}{T_1} - \frac{1}{T_2}\right) \quad (23)$$

Where the factor (A) is pre-exponential, E_a activation energy, K is the rate constant of reaction and R is the ideal gas constant. The plot is $\ln(k)$ vs $1/T$ gives a slope representing $\frac{E_a}{R}$ [27].

Adsorbents derived from *Moringaoleifera* pods have been used in the reduction of chromium in wastewater [28]. In this study, adsorptive properties of pyrolyzed and characterized (Part A) *Moringaoleifera* seed pods and shells was investigated with variables from adsorption isotherms, kinetics, and thermodynamics. Tannery effluent from NILEST, Zaria, and chromium ion is the medium and adsorbate respectively.

Materials and Methods

The chromium concentration was determined using a Zeenit 700 absorption spectrometer (Germany) coupled with a flame atomizer and a chromium hollow cathode lamp. AROSTEK Instrument column chromatography was used for the column studies. It has a diameter of 9-10 mm with a maximum loading capacity of 0.1 g.

The Adsorbent

Moringaoleifera seeds were obtained from Lafia central market, Nigeria and presented for identification at the Botany Department of the University of Agriculture Makurdi, Nigeria. The pods were de-seeded and collected as the precursor for PMOP, the seeds were de-shelled and the shells were washed with water, dried at room temperature and stored for use as starting material for PMOS. Both dried pods and shells were pulverized and pass through a < 2 mm size sieve and carbonized [29]. The stages include washing, air drying, and oven drying. Heating was conducted in a muffle furnace at 400°C for 8 hours. Samples were cooled to room temperature and washed to remove residual ash until constant pH of 6-7 was reached. The washed pyrolyzed sample was oven

dried at 105°C to constant weight. The final products were kept in an airtight polyethylene bag [30] and labeled accordingly as “ pyrolysed *Moringaoleifera* pods (PMOP)” and “ pyrolysed *Moringaoleifera* shells (PMOS)” for further analysis.

The Adsorbate

Tannery wastewater was collected from Nigerian Institute of Leather and Science Technology (NILEST) of coordinates; Latitude 11.16670, Longitude 7.63330. Effluent collection [31,33] was carried out, first by stirring before lowering a clean 4L glass bottle (previously washed with 0.1 M HNO₃) into different depths (15 cm). Sample overflow bottle was withdrawn and stored at 4 °C for further analysis.

Effluent Digestion for AAS analysis

A Procedure [33] was followed. 10 mL of 1:1 HNO₃ was mixed with the tan-chrome liquor (2 mL). The mixture was heated to 95 °C ± 5 °C and reflux for 10 to 15 minutes without boiling. The mixture was allowed to cool followed by addition of 5 mL of concentrated HNO₃, cooling for 30 minutes until the generation of brown fumes (oxidation) by HNO₃. Digestion was repeated with the addition of 5 mL of conc. HNO₃ over and over until no brown fumes were given off by the sample indicating the complete reaction with HNO₃. The solution was allowed to evaporate to approximately 5 mL. The digest was filtered using a Whatman No. 41 and the filtrate collected in a 100 mL volumetric flask. The digested tannery effluent was analyzed with AAS to determine chromium.

Description and Preparation of column

A Rostek column Instrument with diameter 9-10 mm and Max loading of 100 mg (0.1g) was used. It was clapped on a retort stand vertically. The column was washed severally with distilled water and dried in an oven. A piece of cotton was carefully tucked into the glass column close to the tap. This is to ensure that the adsorbents don't block the column and also to ensure the eluent is collected without the adsorbents. The needed weight of the adsorbents was weighed (bed depth was noted) and carefully placed in the column. It was tapped to remove trapped air. The set up was wet with distilled water and set for usage. The tannery effluent was poured from the top while the eluent was collected from the tap.

Isotherm Studies

The adsorbent was utilized to adsorb Cr (VI) of different adsorbate (chromium) concentration (200 – 1000 mg/L), pH value of 6, 30 ± 2°C, 0.05 g adsorbent dose and 60 minutes adsorbent/adsorbate

contact time. Made equilibrium data were fitted into four isotherm models. The eluate was collected in sample bottles, labeled and stored for AAS analysis.

Kinetic Experiment

The method used by Vaishali and Dinesh [34] was applied. This involved varying the contact time of the Tan-chrome liquor with the adsorbents in the order of 20 min, 40 min, 60 min, 80 min and 100 min. Parameters which are kept constant are initial concentration; 600 mg/L for PMOS and PMOP, a dosage of 0.05 g, pH of 6.0 volume of 0.025 mg/L and temperature of $30 \pm 2^\circ$. Data generated from kinetic experiments were used to model the modes of transport.

Thermodynamic Experiment

The method used by Gueu, *et al.*[35], was adopted. The temperature of the Tan-chrome liquor was varied (10, 20, 30, 40, and 50°C). All other parameters (pH, initial concentration, dosage, volume and contact time) were kept constant. The eluate was collected in sample bottles, labeled and stored for analysis using AAS.

Results and Discussion

Results obtained for the characterization studies; SEM, TEM, PXRD, FTIR and CHNS/O were presented and reported elsewhere [36]. An investigation of the effects of parametric factors has been reported [36].

Adsorption Isotherms

The relationship between the amount of a substance adsorbed per unit mass of adsorbent at a constant temperature and its concentration in the equilibrium solution is called adsorption isotherm. Adsorption isotherm is important to describe how solutes interact with sorbents. Developing an appropriate model for adsorption is essential to the design and optimization of adsorption processes. Data generated were fitted against four isotherm models namely; Langmuir, Freundlich, Temkin, and Dubinin-Radushkevich [37]. Results were discussed as follows.

Langmuir isotherm: A linear plot was obtained when C_e/q_e was plotted against C_e over the entire concentration range of chromium investigated. R^2 value of 0.7066 for PMOP and 0.8609 for PMOS which showed a good applicability of the model could indicate a monolayer adsorption and homogeneous surface conditions [38]. In Langmuir theory, the basic assumption is because of the fact that the sorption takes place at specific homogeneous sites within the adsorbent. The essential feature of the Langmuir isotherm is a dimensionless constant separation factor (RL). In this context, lower RL value reflects that adsorption is more favorable. In this study, RL value indicates the

adsorption nature to be either unfavorable ($RL > 1$), linear ($RL = 1$), favorable ($0 < RL < 1$) or irreversible ($RL = 0$). The result from this work shows favorable adsorption for PMOS and PMOP which is in agreement with another report [39]. The result showed a better applicability for PMOS than PMOP.

Freundlich isotherm The equilibrium data for chromium over the concentration range of 200 to 1000 mg/L respectively at 30 °C has been modeled with the Freundlich isotherm. The value of $n < 1$ implied an interaction with high strength. Alternately, $n > 1$ suggests multiple binding sites [40]. The correlation coefficient values for Freundlich model indicated suitability (R^2) for PMOP and PMOS. The better fitting of these data into Freundlich isotherm than Langmuir model supports heterogeneous energy distribution [41].

Temkin isotherm: Correlation coefficient values of Temkin indicates that Temkin was not a suitable model with a correlation coefficient, (R^2 of PMOS (0.3652), PMOP(0.3645))

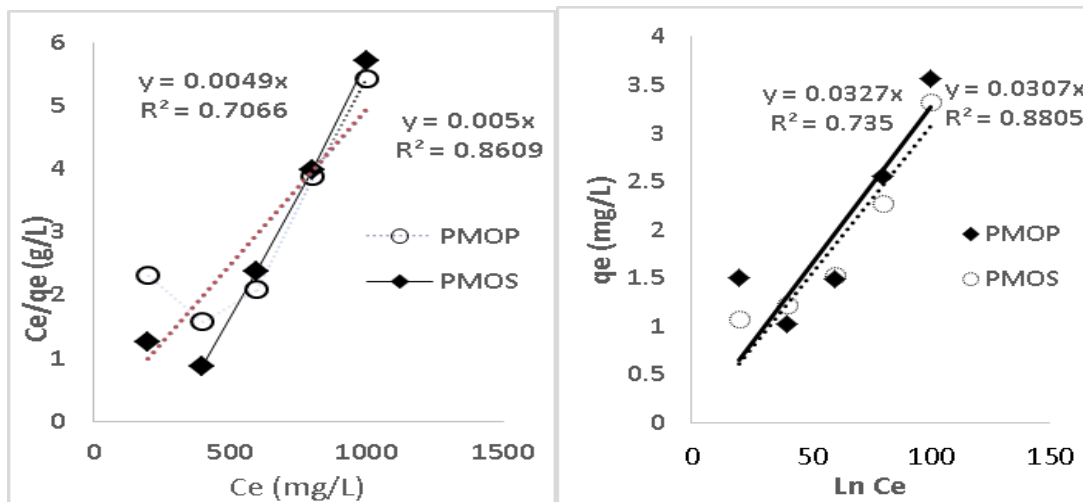


Figure 1. Langmuir and Temkin isotherm plots for chromium adsorption on pyrolyzed MOS and MOP adsorbents.

Table 2. Isotherm Parameters for Chromium onto the Adsorbents

Isotherms	Constant/units	PMOP	PMOS
Langmuir	q_o	333.3	71.4
	K_L	0.003	0.001
	R_L	0.23	0.37
	R^2	0.8609	0.7066
Freundlich	$K_F(mg/g)$	0.8166	0.827
	$1/n$	0.88	1.66
	R^2	0.918	0.8213
Temkin	$b_T(kj/mol)$	0.0327	0.0307

	K_T	0	0
	R^2	0.735	0.8805
Dubinin-Radushkevich	$q_D (mg/g)$	1.4781	1.4601
	E	1.37	1.42
	R^2	-0.958	-0.942

Dubinin–Radushkevich isotherm: The parameters were obtained by plotting $\ln q_e$ vs. ε^2 . The low value of E_a is expected for physisorption. The model assumed that surface coverage could be heterogeneous, to further supports the surface heterogeneity predicted by Freundlich model in this study. However, negative correlation coefficient values of Dubinin–Radushkevich indicates that the model gave the least suitable correlation coefficient, R^2 for PMOS (-0.942), PMOP (-0.958).

Temkin Isotherm: Low values (0.0327 and 0.0307 kJ/mol) reported for the heat of adsorption, b_T also suggests physisorption characterized by a decrease sorption energy with coverage due to adsorbent-adsorbate interactions [17]. The Temkin correlation of applicability (R^2) values also represents the good fit to give an explanation on sorption energies.

Adsorption Kinetic Studies

The study of adsorption kinetics describes the solute uptake rate and evidently, this rate controls the residence time of adsorbate uptake at the solid-solution interface. Taha *et al.* [42] inferred that a kinetic model helps in the study of adsorption rate, model and the process and predicts information about adsorbent/adsorbate interaction (physisorption or chemisorption). The linearity of the second order kinetics for the adsorbents is relatively higher with R^2 for PMOS (0.9540) and PMOP (0.94). Pseudo-second order kinetic proved to be effective in representing the experimental kinetic data for the adsorption by most of the adsorbents. This suggests that chemical reaction plays significant role in the sorption process.

High applicability coefficient (0.9849 and 0.9987) from the Elovich plots assumes a logarithmic time dependence of the adsorbed aqueous phase heavy metal concentrations. The initial desorption rate constants, β were estimated as 1.307 and 0.865 for PMOP and PMOS respectively.

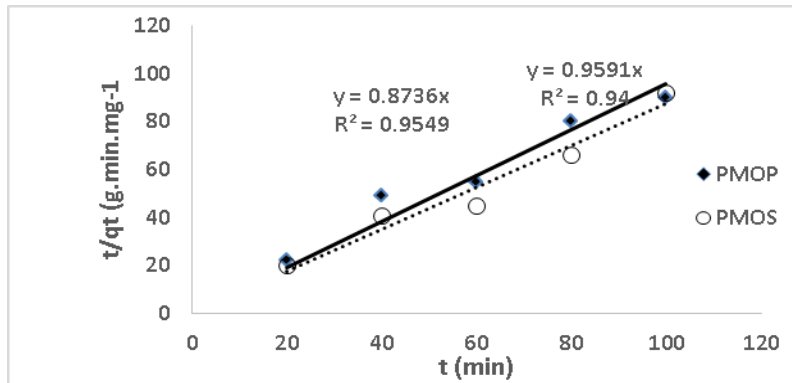


Figure 2. Pseudo-second-order kinetics for chromium adsorption on PMOS and PMOP adsorbents

Table 3. Adsorption kinetic experimental parameters and constants

Kinetics models	Constants	PMOP	PMOS
Pseudo-First Order	q_e,exp	28.14	27.00
	K_1	0.020	0.024
	$q_e(cal)$	50.00	41.67
	R^2	0.7816	0.9710
Pseudo-Second Order	$q_e(cal)$	1.78×10^3	273.42
	K_2	0.01	0.0002
	R^2	0.940	0.9540
Elovich	R^2	0.9849	0.9987
	β	0.865	1.309

Transport Studies

The intra-particle diffusion model, as well as Liquid film diffusion models, were used to investigate if transport of metal ions from the liquid phase to the solid phase boundary plays a role in the adsorption process. Figure 3 shows intra-particle diffusion and film diffusion plots for chromium on PMOS. It is obvious from the very low R^2 value for PMOS(0.8744), PMOS (0.8109) that the boundary layer has a less significant effect on the diffusion of Cr uptake on the adsorbents[43]. The linear plot of q_e vs. $t^{0.5}$ with intercept deviates from zero. This implied that intraparticle diffusion alone does not determine the overall rate of adsorption. In other words, the plots not passing through origin indicate that the tested intra-particle diffusion model is not the only rate controlling factor [44,45].

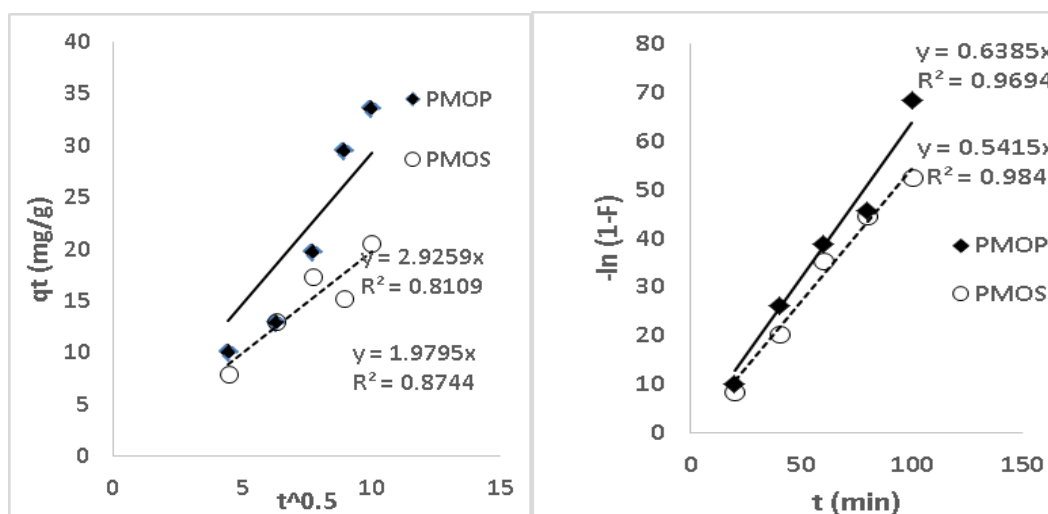


Figure 3. Intra-particle diffusion (LHS) and the Film diffusion model (RHS) for Chromium adsorption on pyrolyzed MOS and MOP adsorbents

The liquid film diffusion model plots of $\ln(1-F)$ versus time were estimated for Cr and presented. The coefficient of regression (R^2) for PMOS (0.984), PMOP (0.9694) was high, implicating film diffusion as most probable rate deciding factor in the adsorption process. This model describes moving adsorbate across the external liquid film to the external surface sites on the adsorbent particles[46]. The intercept values for all the adsorbent are higher than zero but close to the origin. More of such was earlier reported [46]

Table 4. Transport (Diffusion) parameters and constants

Transport models	Constants	PMOP	PMOS
Intra-particle diffusion	R^2	0.8109	0.8744
	K_{1D}	0.020	0.024
	$C_i(mg/L)$	50.00	41.67
Film diffusion	$q_e(cal)$	1.78×10^{33}	273.42
	K_2	0.01	0.0002
	R^2	0.984	0.9694

Thermodynamic studies of chromium adsorption

Figure 4 shows the Van'tHoff Plots of thermodynamic studies for chromium adsorption on PMOS and PMOP adsorbents. It has kept that with an increase in temperature, adsorption capacity decreases. This implies that for the initial tannery effluent concentration of each solution, the adsorption is exothermic in nature. The thermodynamic parameters change in Gibb's free energy (ΔG°), change in enthalpy ΔH° , and change in entropy ΔS° for the adsorption of Chromium over PMOS and PMOP was determined. The positive value for the enthalpy change, ΔH° for the adsorbents indicates endothermic nature of the adsorption, which explains the increase of

Chromium adsorption efficiency as the temperature increased until equilibrium is attained. The positive value for the PMOS entropy change, ΔS° suggests an increased disorder at the solid/liquid interface during Cr adsorption onto the adsorbents. Free energy change (ΔG°) shows that the adsorption process of Chromium was endothermic and non-spontaneous. A similar report has been documented [47].

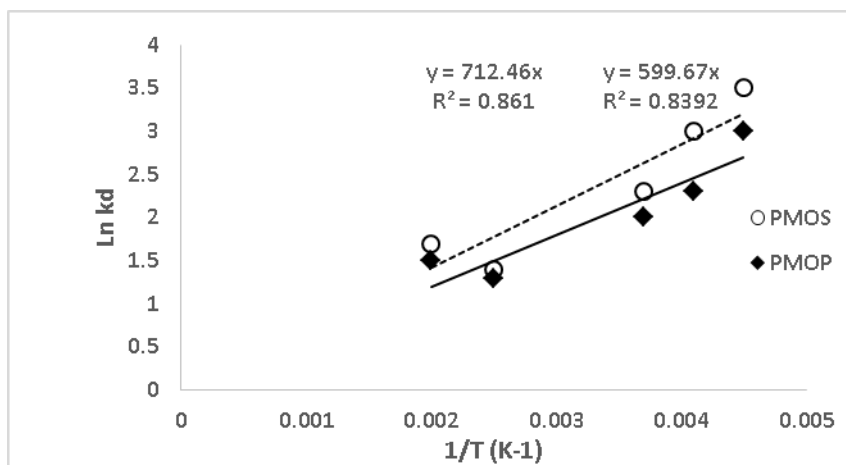


Figure 4. Van't Hoff Thermodynamic Plot for Cr Adsorption onto Pyrolysed MOS and MOP

Table 5. Thermodynamic experimental parameters and constants

Parameters	PMOS	PMOP
R^2	0.861	0.8392
ΔS (kJ/mol)	-0.154	+0.565
ΔH (KJ/mol)	+712.46	+599.67
ΔG (KJ/mol.k)	+716.31	+585.55

Conclusion

Potential adsorbents from *Moringaoleifera* seed shells and pods were prepared, characterized, utilized and compared to their sorptive properties. The comparable level of percentage removal, adsorption capacity and adsorptive properties using the derived adsorbents is a signal of the potential applicability of the pyrolysed *Moringaoleifera* pods and shells as adsorbents. The equilibrium and Kinetic studies show that the adsorption of Cr from tannery effluent is best modeled using pseudo-second-order kinetics with film diffusion as the most plausible transport mechanism.

References

[1]. Jaap K., *Small-scale techniques and management*, TOOL, 1999, Amsterdam.

- [2]. Rameshraj D., Suresh S., *Int. J. Env. Res.*, 2010, **5**:349
- [3]. Covington A.D. *Chem. Soc. Rev.*, 1997, **25**:111
- [4]. Malek A., Hachemi M., Didier V. *J. Hazar. Mater.*, 2009, **170**:156
- [5]. Miretzky P., Cirelli A.F. *J. Hazar. Mater.*, 2010, **180**:1
- [6]. Gupta V.K., Jain R., Nayaka A., Agarwal S., Shrivastava M. *Mater. Sci. Engin.*, 2011., **31**:1062
- [7]. Ghaedi M., Sadeghian B., Pebdani A.A., Sahraei R., Daneshfar A., Duran, C. *Chem. Engin. J.*, 2012, **187**:133
- [8]. Saleh T.A., Gupta V.K. *J. Coll. Interface Sci.*, 2012, **371**:101
- [9]. Adamson, A.W. *Physical Chemistry of Surfaces*, 5th ed., John Wiley & Sons, New York: **1990**, 67
- [10]. Demirbas E., Kobya M., Sulak M.T., *BioresourcesTechnology*, 2008, **99**:5368
- [11]. Pandey P.K., Sharma S.K., Sambhi S.S. *Int. J. Environ. Sci. Tech.*, 2011, **7**:395
- [12]. Sharma P., Kumari P., Srivastava M.M., Srivastava S., *Bioresource Technology*, 2006, **97**:299
- [13]. Arnoldsson E., Bergman M., Matsinhe N. *Int. J. Adv. Res.*, 2008, **4**:124
- [14]. Wang S., Li L., Wu H., Zhu Z.H. *J. Coll. Interface Sci.*, 2005, **292**:336
- [15]. Febrianto J., Kosasih A.N., Sunarso J., Ju Y.H., Indraswati N., Ismadji S., *J. Hazard. Mater.*, 2009, **162**:616
- [16]. Reddy D.H.K., Harinath Y., Seshaiiah K., Reddy A.V.R. *Chem. Engin. J.*, 2010, **162**:626
- [17]. Arasakumar A., Arivoli S., Marimuthu V., *Int. J. Latest Res. Sci. Tech.*, 2017, **6**:32
- [18]. Allen S.J., McKay G., Porter J.F. *Journal of Colloid Interface Science*, 2004, **280**:322
- [19]. Zohre S., Ataallah S.G., Mehdi A. *Journal of Water Resources Development*, 2010, **2**:016
- [20]. Chen X., *Information*, 2015, **6**:14
- [21]. Ho Y.S., McKay G., *Trans IChemE*, 1998, **76**:183
- [22]. Blanchard G., Maunaye M., Martin G., *Water Res.*, 1984, **18**:1501
- [23]. Crittenden J.C., Berrigan J.K. Hand D.W. *Journal of Environmental. Engineers*, 1987, **113**:243
- [24]. Tarawou T., Young E. *International Research Journal of Engineering and Technology*, 2015, **2**:239
- [25]. Nwabanne J.T., Igbokwe P.K. *Advances in Applied Science Research*, 2011, **2**:166
- [26]. Parimalam R., Raj V., Sivakumar P. *Journal of Engineering and Applied Sciences*, 2011, **6**:19
- [27]. Keith J. *Journal of chemical Education*, 1984, **6**:494
- [28]. Sulyman A.S., Bello Y.I., Akanni H.I., Oniwapele A.S., Muktari M. *Journal of Environmental Science, Toxicology and Food Technology*, 2015, **9**:96
- [29]. Adowei P, Horsfall M., Spiff A.I. *Innovation Science Engineers*, 2012, **2**:24
- [30]. Tarawou T., Horsfall M., Jose V.L. *Chemistry Biodiversity*, 2007, **4**:2236

- [31]. Kawser A.M., Monika D., Islam M.M., Mosammat S.A., Shahidul I., Muhammad A.A.M. *World Applied Sciences Journal*, 2011, **12**:152
- [32]. Islam B.I., Musa A.E., Ibrahim E.H., Salma A.A., Elfaki B.M., *Journal of Forest Products & Industries*, 2014, **3**:141.
- [33]. Edgell K. USEPA, **1988** No. 68-03-3254.
- [34]. Vaishali T., Dinesh K. *Chemistry Central Journal*, 2013, **7**:1
- [35]. Gueu B.S., Yao K., Adouby G.A., *International Journal of Environmental Science and Technology*, 2007, **4**:11
- [36]. Itodo A.U., Wuana R.A., Wombo N.P. (Under review), *Chemical methodology*, **2018**
- [37]. Salleh M.A., Mahmoud K.D., Karim W.A., Idris A. *Desalination*, 2011, 280:1.
- [38]. Vinodhini V., Das N. *International Journal of Environmental Science and Technology*. 2010, **7**:85
- [39]. Hameed B.H., Foo K.Y. *Chemical Engineering Journal*, 2010, **156**:2
- [40]. Chiou M.S., Li H.Y. *J. Hazard. Mater.*, 2002, **93**:233
- [41]. Riemam W., Walton H. *Ion exchange in analytical chemistry*, 1970, **1970**:38.
- [42]. Taha M., Ismail N.H., Jamil W., Rashwan H., Kashif S.M., Sain A.A., Adenan M.I., Anouar E.H., Ali M., Rahim F., Khan K.M. *Synthesis of novel derivatives*, **2014**.
- [43]. Mohanta M., Salam M.A., Saha A.K., Hasan A., Roy A.K., *Asian Journal of Experimental Biological Science*, 2010, **2**:294
- [44]. Suguna M., Siva K. ., Venkata S.M., Krishnaiah A. *Journal of Chemical and Pharmaceutical Research*, 2010, **2**:7
- [45]. Itodo A.U., Abdulrahman F.W., Hassan L.G., Maigandi S.A., Happiness U.O. *Iranian Journal of Chemistry and Chemical Engineering*, 2011, **30**:51
- [46]. Choy K.K.H., Ko D.C.K., Cheung C.W., Porter J.F., McKay G. J. *Coll. Interface Sci.*, 2004, **271**:284
- [47]. Srivastava V.C., Mall I.D., Prasad B., Mishra I.M. *Colloids and Surfaces, Engineering Aspects*, 2006, **272**:89
- [48]. Azraa A., Jain K., Tong K.S., Rozaini C.A., Tan L.S. *J. Phy. Sci.*, 2012, **23**:1

How to cite this manuscript: Adams Udoji Itodo*, Raymond Ahulle Wuana, Wombo Ngunan Patience. On The Characterization, Use and Wastewater Detoxification Potential of Pyrolyzed *Moringaoleifera* Pods and Shells, PART B: Sorption Isotherm, Kinetic, and Thermodynamic study. *Chemical Methodologies* 2(2), 2018, 166-180. DOI: [10.22631/chemm.2018.113853.1033](https://doi.org/10.22631/chemm.2018.113853.1033).